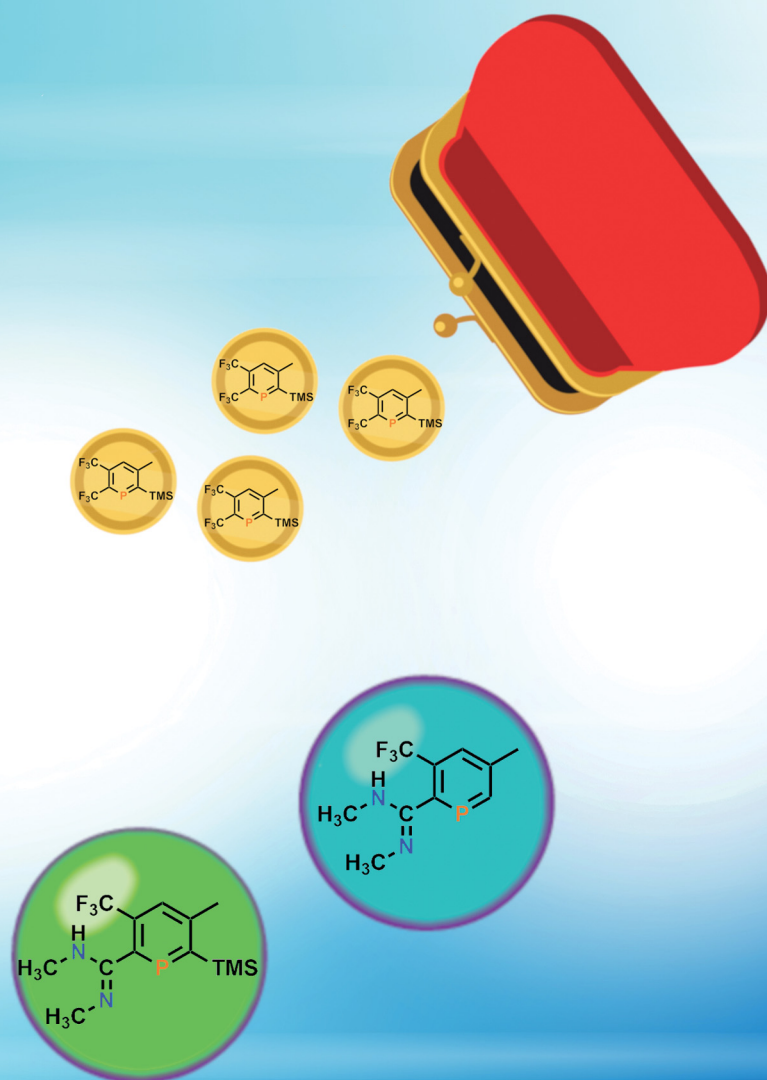
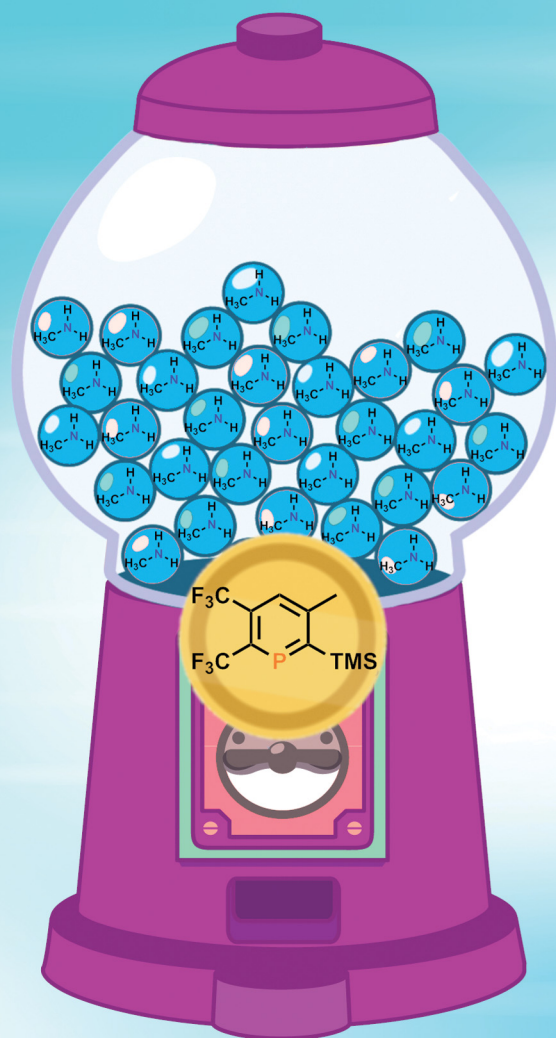


# ChemComm

Chemical Communications

rsc.li/chemcomm



ISSN 1359-7345

## COMMUNICATION

Nathan T. Coles, Samuel E. Neale, Christian Müller *et al.*  
Triple dehydrofluorination as a route to amidine-functionalized,  
aromatic phosphorus heterocycles


 Cite this: *Chem. Commun.*, 2022, 58, 13580

 Received 20th September 2022,  
 Accepted 3rd November 2022

DOI: 10.1039/d2cc05178h

rsc.li/chemcomm

# Triple dehydrofluorination as a route to amidine-functionalized, aromatic phosphorus heterocycles†‡

 Nathan T. Coles,<sup>a</sup> Lucie J. Groth,<sup>a</sup> Lea Dettling,<sup>a</sup> Daniel S. Frost,<sup>a</sup> Massimo Rigo,<sup>a</sup> Samuel E. Neale<sup>b</sup> and Christian Müller<sup>b,c</sup>

**An unexpected route to hitherto unknown amidine-functionalized phosphinines has been developed that is rapid and simple. Starting from primary amines and CF<sub>3</sub>-substituted λ<sup>3</sup>,σ<sup>2</sup>-phosphinines, a cascade of dehydrofluorination reactions leads selectively to ortho-amidinephosphinines. DFT calculations reveal that this unusual transformation can take place via a series of nucleophilic attacks at the electrophilic, low-coordinate phosphorus atom.**

λ<sup>3</sup>,σ<sup>2</sup>-Phosphinines, also known as phosphabenzenes, are aromatic phosphorus heterocycles which are currently undergoing an intriguing renaissance in the fields of coordination chemistry, homogeneous catalysis, activation of small molecules and photoluminescent molecular materials.<sup>1</sup> Our group and others have previously developed a number of (donor-)functionalized λ<sup>3</sup>- and λ<sup>5</sup>-phosphinines, which are of particular relevance for their use in such research fields and a brief selection (I–VI) is depicted in Fig. 1.<sup>2–7</sup> In this respect, the specific functionalization of phosphinines is of particular importance in order to modify their stereoelectronic properties.

During the course of our investigations on [4+2]-cycloaddition reactions on phosphinines, we found not only a synthetic access to hitherto unknown CF<sub>3</sub>-substituted phosphinines, but also an unexpected series of dehydrofluorination reactions in the presence of primary amines, that yielded novel amidine-substituted phosphinines selectively (Fig. 1).

We have previously synthesized 1-phosphabarrelene **2b** from phosphinine **1b** in the presence of hexafluoro-2-butyne, which has now been expanded to **1a/2a** (Scheme 1).<sup>8</sup> Gratifyingly, we were able to characterise the known phosphinine **1a**<sup>9</sup> and the novel phosphabarrelene **2b** also crystallographically (Fig. S92 and S93, ESI†).

Interestingly, we noticed that upon heating a toluene solution of **2a/b** in a high-pressure reaction vessel to *T* = 200 °C, a retro-Diels–Alder reaction occurs, leading selectively to trifluoromethyl substituted phosphinines **3a/b**. For **3b**, crystals suitable for an X-ray crystallographic analysis, were obtained by storing the oily sample at *T* = –20 °C. The molecular structure of **3b** (Fig. S94, ESI†) in the solid state confirms the presence of the retro-Diels–Alder product. Notably, this reactivity has never been observed in the chemistry of phosphinines and phosphabarrelenes before. It offers the exceptional possibility to introduce electron withdrawing CF<sub>3</sub> groups to a phosphinine core in a facile manner.<sup>10</sup> Consequently, we were interested in exploring the effect of the CF<sub>3</sub> substituents on the energy levels of the frontier molecular orbitals (MOs) of **3a/b** first.

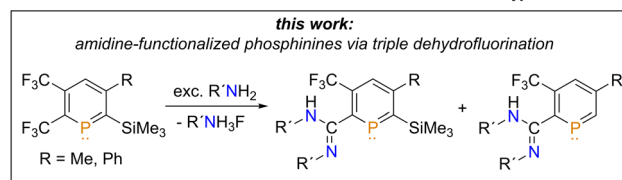
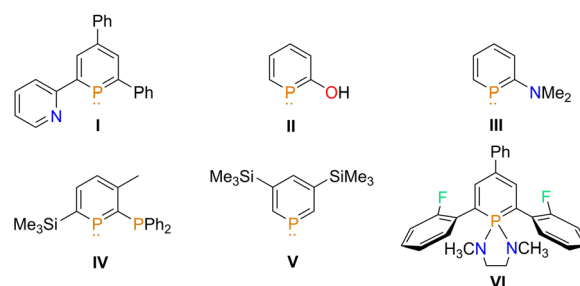


Fig. 1 Selected functionalized λ<sup>3</sup>- and λ<sup>5</sup>-phosphinines and brief summary of this work.

<sup>a</sup> Institute of Chemistry and Biochemistry, Freie Universität Berlin, Fabeckstr. 34/36, 14195 Berlin, Germany. E-mail: c.mueller@fu-berlin.de

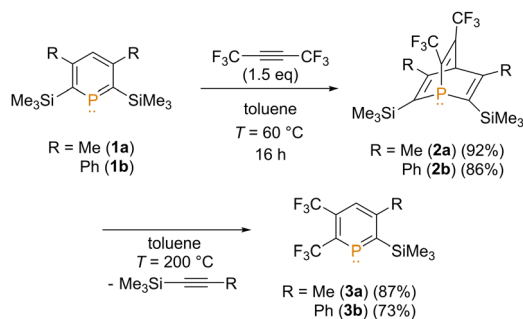
<sup>b</sup> School of Chemistry, University of Nottingham, University Park, Nottingham NG7 2RD, UK. E-mail: Nathan.Coles@nottingham.ac.uk

<sup>c</sup> Department of Chemistry, University of Bath, Claverton Down, Bath BA2 7AY, UK. E-mail: sen36@bath.ac.uk

† Dedicated to Prof. Dr Evamarie Hey-Hawkins on the occasion of her 65th birthday.

‡ Electronic supplementary information (ESI) available. CCDC 2176809–2176812. For ESI and crystallographic data in CIF or other electronic format see DOI: <https://doi.org/10.1039/d2cc05178h>





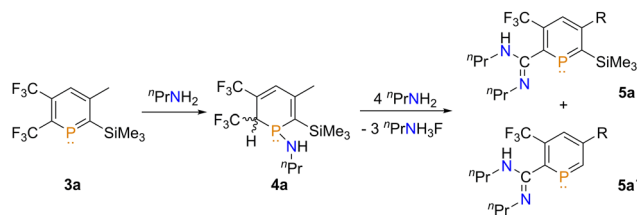
**Scheme 1** Synthesis of phosphininines **3a/b** via selective cycloaddition-cycloreversion reaction.

The introduction of  $\text{SiMe}_3$ -groups at the *ortho*-position of the aromatic phosphorus heterocycle increases the energy of the occupied MOs.<sup>11</sup> Most notably, there is a significant increase in the energy level of the lone-pair (HOMO-1), with respect to the parent phosphininine  $\text{C}_5\text{H}_5\text{P}$  (HOMO-2), while the energy levels of the respective LUMOs do not change significantly (Fig. S97, ESI $\ddagger$ ). For **3b**, the HOMO-3 represents now the lone-pair at the phosphorus atom, which is at a comparable energy level to the one of the parent phosphininine. In clear contrast, the LUMO of **3b** has the character of an empty p-orbital at the phosphorus atom and is stabilized by almost 0.6 eV with respect to the unsubstituted phosphininine, which renders the low-coordinate phosphorus atom much more electrophilic. In this respect, the orientation of the relevant molecular orbitals (HOMO-3 and LUMO) is similar to the situation found in carbenes.

It is well documented that strong nucleophiles, such as organolithium compounds, react at the phosphorus atom to afford 1-*R*-phospha-cyclohexadienyl anions, also known as  $\lambda^4$ -phosphininines.<sup>12</sup> Due to the energetically low-lying LUMO we anticipated that **3a/b** might also react with much less nucleophilic amines, which could lead to interesting follow-up reactions at the phosphorus heterocycle. Initial reactivity studies were performed with **3a** and  ${}^n\text{PrNH}_2$ . Using two equivalents of  ${}^n\text{PrNH}_2$  in DCM, a small new signal at  $\delta(\text{ppm}) = 0.3$  in the  ${}^{31}\text{P}\{^1\text{H}\}$  NMR spectrum was observed (Fig. S1, ESI $\ddagger$ ). The signal appears as a quartet with a coupling constant of  ${}^3J_{\text{P-F}} = 19.0$  Hz, which is substantially smaller with respect to the starting material ( ${}^3J_{\text{P-F}} = 53.0$  Hz). We tentatively assigned this resonance to compound **4a** (Scheme 2).

The formation of **4a** is also corroborated by a large chemical shift difference of  $\delta(\text{ppm}) = 245.3$ , leading to a shift of  $\delta(\text{ppm}) = 1.6$  in the  ${}^{31}\text{P}\{^1\text{H}\}$  NMR spectrum (**3a**: single resonance at  $\delta(\text{ppm}) = 245.6$  in  $\text{CDCl}_3$ ). The  ${}^{19}\text{F}$  NMR spectrum of **4a** (Fig. S2, ESI $\ddagger$ ) shows two new signals at  $\delta(\text{ppm}) = -65.0$  (m) and  $\delta(\text{ppm}) = -66.4$  (br, s), which had shifted from  $\delta(\text{ppm}) = -52.9$  and  $\delta(\text{ppm}) = -59.4$ , respectively, compared to **3a**. Interestingly, when the solvent was removed and replaced by THF and some additional  ${}^n\text{PrNH}_2$  and left to stand overnight, a substantial change to the  ${}^{31}\text{P}\{^1\text{H}\}$  NMR spectra was noticed (Fig. S3, ESI $\ddagger$ ).

Next to **3a** and **4a**, as well as protodesilylated starting material (**3a'**, Fig. S3, ESI $\ddagger$ ), signals at  $\delta(\text{ppm}) = 214.1$  (s) (**5a**)



**Scheme 2** Reaction of **3a** with  ${}^n\text{PrNH}_2$  showing the equivalents of amine that has been introduced into the phosphininine. **4a** synthesised using 10 equivalents of  ${}^n\text{PrNH}_2$ . **5a/a'** synthesised using an excess of  ${}^n\text{PrNH}_2$ .

and  $\delta(\text{ppm}) = 242.4$  (s) (**5a'**) which could not be assigned initially. The  ${}^{19}\text{F}$  NMR spectrum of the reaction mixture (Fig. S4 and S5, ESI $\ddagger$ ) showed two new singlets at  $\delta(\text{ppm}) = -61.9$  (**5a'**) and  $\delta(\text{ppm}) = -62.2$  (**5a**) alongside a singlet at  $\delta(\text{ppm}) = -154.6$ . Remarkably, the two new singlets in the  ${}^{19}\text{F}$  NMR spectrum were both found in a region similar to that observed for the *meta*- $\text{CF}_3$  of **3a** ( $\delta(\text{ppm}) = -61.1$ ) and **3a'** ( $\delta(\text{ppm}) = -60.9$ ). The  ${}^{19}\text{F}$  data coupled with the observations in the  ${}^{31}\text{P}\{^1\text{H}\}$  spectra suggested that a chemical transformation had occurred exclusively at the  $\text{CF}_3$  moiety adjacent to the phosphorus atom (Scheme 2).

With these initial results attempts were made to cleanly synthesize **5a** and **5a'**. By increasing the equivalents of amine from two to ten the reaction became faster, with  $\approx 80\%$  conversion to **4a** by  ${}^{31}\text{P}\{^1\text{H}\}$  and  ${}^{19}\text{F}$  NMR spectroscopy in only 30 minutes (Fig. S6 and S7, ESI $\ddagger$ ). Leaving this sample for 20 hours led to most of **4a** being consumed, with **5a** and **5a'** being the major species (Fig. S8 and S9, ESI $\ddagger$ ). Visually, the samples became extremely viscous with a large amount of precipitate forming, which was later confirmed as  ${}^n\text{PrNH}_3\text{F}$ . Increasing the temperature to  $T = 60$  °C with ten equivalents of amine led to a larger proportion of **5a'** relative to the reaction at room temperature (Fig. S10, ESI $\ddagger$ ). Leaving this sample for 2 months at room temperature caused a complete loss of the signal for **5a** (Fig. S12, ESI $\ddagger$ ). In the  ${}^{19}\text{F}$  NMR spectrum, a signal attributed to **5a'** was observed along with the characteristic signal of  $\text{FSiMe}_3$  at  $\delta(\text{ppm}) = -154.6$ . This observation indicates that  ${}^n\text{PrNH}_3\text{F}$  is generated during the course of the reaction, which over time initiates the protodesilylation reaction. The formation of the **5a/5a'** could be halted by removal of the excess amine after **4a** had formed. The  ${}^1\text{H}$  NMR spectrum of **4a** shows a substantial upfield shift for the proton at the *para*-position of the heterocyclic ring ( $\delta(\text{ppm}) = 0.66$  to  $\delta(\text{ppm}) = 6.60$ ). Other characteristic signals occur at  $\delta(\text{ppm}) = 3.52$  ppm and  $\delta(\text{ppm}) = 2.24$ – $2.08$ . The signal at  $\delta(\text{ppm}) = 3.52$  can be attributed to a proton adjacent to the *ortho*- $\text{CF}_3$  group as it appears as a quartet of doublets, caused by coupling to both  ${}^{19}\text{F}$  and  ${}^{31}\text{P}$  nuclei.

With these findings in mind, an attempt was made to form **5a** selectively by using a vast excess of amine. This was implemented to shorten the reaction time and try to prevent the protodesilylation of the  $\text{SiMe}_3$ -group due to the limited solubility of the ammonium salt. Gratifyingly, using 0.1 mL of benzene, to help dissolve **3a** (0.13 mmol), with 0.5 mL of  ${}^n\text{PrNH}_2$  led initially to the formation of the  $\text{SiMe}_3$ -substituted



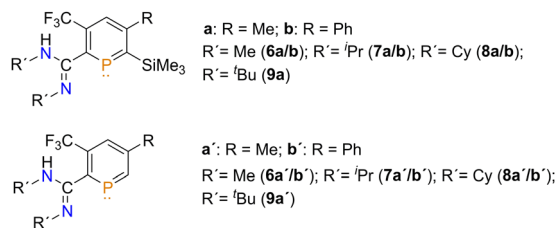


Fig. 2 Substrate scope for the novel triple dehydrofluorination reaction.

phosphininine, with a conversion of greater than 90%. After filtering the solution to remove the ammonium salt and removal of the volatiles, the residual oil was dissolved in  $\text{C}_6\text{D}_6$ . A spectroscopic yield of 47% was obtained against an internal standard ( $\text{PPh}_3$ ). However, upon filtering, some protodesilylation was observed by means of NMR spectroscopy, most likely due to traces of dissolved  $^t\text{PrNH}_3\text{F}$  during the isolation of the product.

In order to fully identify the reaction products, the substrate scope of this reaction was further expanded to other amines (Fig. 2 and Scheme S1, ESI $\ddagger$ ). We first focused on  $\text{MeNH}_2$ . The reaction was performed by condensing dried  $\text{MeNH}_2$  directly onto the phosphininine at  $T = -60^\circ\text{C}$  and stirring at this temperature for 1 hour. Initially, the  $\text{SiMe}_3$ -substituted phosphininine could again be isolated and characterized. However, upon removal of the volatiles and leaving the residue as an oil for 3 days, a crystalline material formed. When the solid was redissolved, only the protodesilylated product could be observed by means of NMR spectroscopy. Again, we believe that traces of  $\text{MeNH}_3\text{F}$  caused the loss of the  $\text{SiMe}_3$  group.

Pleasingly, slow evaporation of a DCM solution of the  $6\text{a}'$  yielded single crystals suitable for single crystal X-ray diffraction. The molecular structure of  $6\text{a}'$  in the crystal, along with selected bond lengths and angles, is given in Fig. 3.

Much to our delight, the crystallographic characterization of  $6\text{a}'$  reveals, that the final product is indeed a protodesilylated, amidine-functionalized phosphininine. The presence of only one  $\text{CF}_3$  group, the fully planar phosphorus heterocycle and the absence of a  $\text{SiMe}_3$ -group is in full agreement with the NMR spectroscopic data of the product(s) described above and depicted already in Scheme 2. In the solid state, at  $T = 100\text{ K}$ , the C–N bonds are found to be at lengths expected for both a

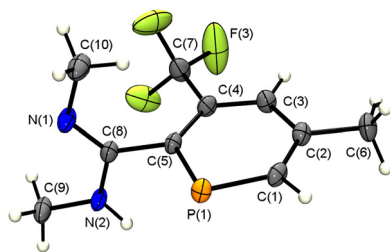


Fig. 3 Molecular structure of  $6\text{a}'$ . Thermal ellipsoids are represented at 50% probability. Selected bond lengths ( $\text{\AA}$ ) and angles ( $^\circ$ ): P(1)–C(1): 1.728(3); C(1)–C(2): 1.390(4); C(2)–C(3): 1.395(4); C(3)–C(4): 1.395(4); C(4)–C(5): 1.392(4); C(5)–P(1): 1.740(3); C(5)–C(8): 1.508(4); C(8)–N(1): 1.288(4); C(8)–N(2): 1.358(4); C(1)–P(1)–C(5): 101.26(15); C(2)–C(3)–C(4): 124.1(3); N(1)–C(8)–N(2): 121.0(3).

$\text{C}=\text{N}$  double bond and a C–N single bond, in contrast to what is observed in solution at room temperature where rapid tautomerization of the amidine takes place, as evidenced by the broad signals for the groups bound to the nitrogen atoms. Interestingly, the amidine group orientates itself perpendicular to the plane of the phosphininine ring. This might allow for intermolecular hydrogen bonding in the solid state (Fig. S96, ESI $\ddagger$ ).

When using aniline, no reactivity towards  $3\text{a}$  was observed, even after 6 days. Both  $^t\text{PrNH}_2$  and  $\text{CyNH}_2$  reacted to give  $7\text{a}/7\text{a}'$  and  $8\text{a}/7\text{a}'$ , respectively.  $^t\text{BuNH}_2$  yielded  $9\text{a}/9\text{a}'$ , however, in this case an unknown impurity accompanied the desired products, which could not be separated. The reactions were also expanded to phosphininine  $3\text{b}$ , resulting in  $5\text{b}$ – $8\text{b}$  (Fig. 2).

This transformation of an aromatic  $\text{CF}_3$  group into an amidine, involving the formal loss of three equivalents of HF was thus considered unusual given that  $\text{CF}_3$ -groups in aryl-trifluorides are normally resistant towards chemical degradation. A few methods for chemical modification of such a group have been developed during the last decade,<sup>13</sup> with some requiring harsh reaction conditions or the presence of strong Lewis acids.<sup>14</sup>  $\text{CF}_3$  groups of activated aromatic rings, for example, have been shown to degrade in the presence of amines and aqueous NaOH, resulting in amides.<sup>15</sup>

The first step appears to be the formal addition of the N–H bond across the  $\text{P}=\text{C}$  double bond.<sup>16</sup> The following steps to the amidine substituent, however, could not be identified experimentally, as no other intermediate species were observed by means of NMR spectroscopy. We therefore employed DFT calculations at the M052X-D3,THF/def2-QZVPP//TPSS/def2-TZVPP level of theory to elucidate the full reaction pathway (see ESI $\ddagger$  for full computational details<sup>17</sup>). The calculations focussed on the triple dehydrofluorination of  $3\text{a}$  (species **I** in the DFT profile) to form  $6\text{a}$  (**VII**), with the computed free energy profile outlined in Fig. 4.

Initial efforts (not shown in Fig. 4) were dedicated to the description of formal N–H bond activation across the  $\text{P}=\text{C}$  bond of the phosphininine and the corresponding product, as the tentative identification of this process was confirmed by NMR spectroscopy. While this process can proceed *via* an accessible activation barrier of +26.0  $\text{kcal mol}^{-1}$  (see Fig. S98, ESI $\ddagger$ ), consistent with the experimental identification of this product, subsequent H–F coupling was disregarded owing to the large computed activation barrier for such a process (+65.2  $\text{kcal mol}^{-1}$ ).

An alternative pathway starting from **I** was in turn identified in which the addition of  $\text{MeNH}_2$  occurs *via* the nitrogen atom at the phosphorus centre, with concomitant H–F coupling. This takes place *via* **TS(I-II)** and a barrier of +31.7  $\text{kcal mol}^{-1}$  to form **II** (+14.3  $\text{kcal mol}^{-1}$ , Fig. 3) indicating that nucleophiles can directly attack the phosphorus LUMO in low-coordinate organophosphorus species under formation of  $\lambda^4$ -phosphinines.<sup>12</sup> In this initial step the unsaturated  $\text{C}=\text{F}_2$  group is formed, where subsequent addition of a second  $\text{MeNH}_2$  at this unsaturated carbon centre, *via* **TS(II-III)** (+32.1  $\text{kcal mol}^{-1}$ ) yields **III** (+26.7  $\text{kcal mol}^{-1}$ ). From **III** the phosphininine heterocycle is exergonically re-aromatized to form **IV** (–6.5  $\text{kcal mol}^{-1}$ ). Subsequent addition of  $\text{MeNH}_2$  at the phosphorus centre allows for another



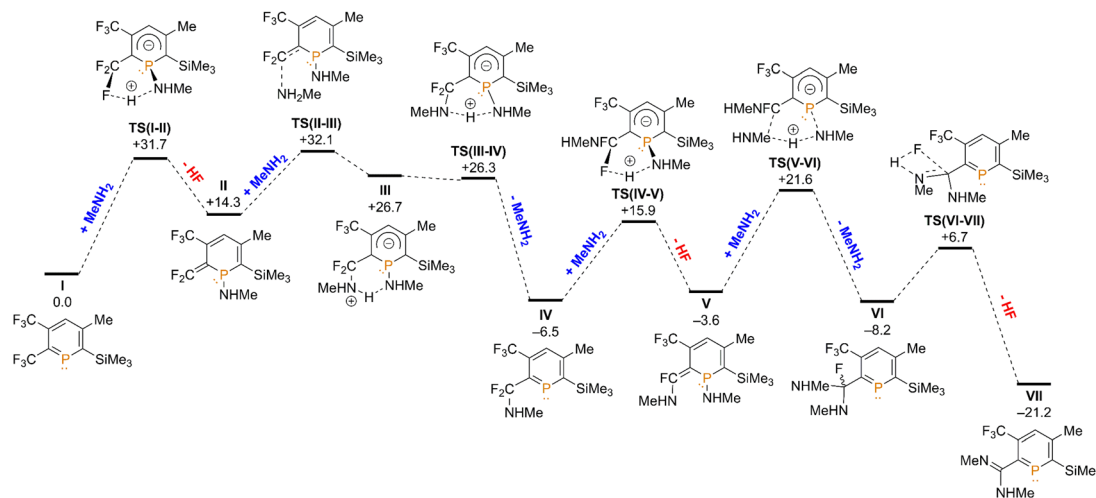


Fig. 4 DFT free energy profile of the triple dehydrofluorination of **3a** (labelled **I** in the profile) with  $\text{NH}_2\text{Me}$ , calculated at the M052X-D3, THF/def2-QZVPP//TPSS/def2-TZVPP level.

process of H-F elimination to yield **V** ( $-3.6 \text{ kcal mol}^{-1}$ ), whereby a repeated process of  $\text{MeNH}_2$  addition to the unsaturated  $\text{MeHNFC}=\text{C}$  moiety with concerted proton transfer eliminates  $\text{MeNH}_2$  from the phosphorus centre and gives the bis-amino-fluoro-substituted species **VI** ( $-8.2 \text{ kcal mol}^{-1}$ ). Dehydrofluorination *via* an H-F coupling from **VI** affords the final amidine product, **VII** ( $-21.2 \text{ kcal mol}^{-1}$ ). Most intriguingly, the DFT calculations verify that the unusual transformation of the *ortho*- $\text{CF}_3$  group to an *ortho*-amidine substituent is feasible owing to the electrophilicity of the low-coordinate phosphorus centre that allows nucleophilic addition of the amine and subsequent elimination of HF.

In summary, a route to hitherto unknown  $\text{CF}_3$ -substituted phosphinines by cycloaddition–cycloreversion reaction on bis- $\text{SiMe}_3$  substituted phosphinines has been developed. These compounds undergo a cascade of dehydrofluorination reactions in the presence of primary amines to form novel amidine-functionalized phosphinines. DFT calculations revealed that the  $\text{CF}_3 \rightarrow$  amidine transformation is driven by a series of nucleophilic additions of the amine to the electrophilic phosphorus centre, which then allows for concerted HF elimination reactions. Phosphinines, decorated with certain functionalities, can thus promote unusual chemical transformations of small molecules. This might also apply for other  $\text{CF}_3$ -substituted organophosphorus compounds containing P-C multiple bonds. Further investigations in this direction and in the coordination chemistry of the here reported novel P,N-hybrid ligands as well as their use in catalytic reactions are currently performed in our laboratories.

C. M. and N. T. C. acknowledge the Deutsche Forschungsgemeinschaft (DFG) for financial support. Dr G. Thiele and C. von Randow are thanked for the supply and handling of dry  $\text{MeNH}_2$ . S. E. N. acknowledges the Anatra HPC service at The University of Bath.

## Conflicts of interest

There are no conflicts to declare.

## Notes and references

- (a) N. T. Coles, A. S. Abels, J. Leitl, R. Wolf, H. Grützmacher and C. Müller, *Coord. Chem. Rev.*, 2021, **433**, 213729; (b) A. Paderina, R. Ramazanov, R. Valiev, C. Müller and E. Grachova, *Inorg. Chem.*, 2022, **61**, 11628; (c) J. Leitl, M. Marquardt, P. Coburger, D. J. Scott, V. Streitferdt, R. M. Gschwind, C. Müller and R. Wolf, *Angew. Chem., Int. Ed.*, 2019, **58**, 15407; (d) X. Chen, Z. Li, F. Yanan and H. Grützmacher, *Eur. J. Inorg. Chem.*, 2016, 633; (e) P. Roesch, J. Nitsch, M. Lutz, J. Wiecek, A. Steffen and C. Müller, *Inorg. Chem.*, 2014, **53**, 9855; (f) J. Moussa, L. M. Chamoreau and H. Amouri, *RSC Adv.*, 2014, **4**, 11539.
- C. Müller, D. Wasserberg, J. J. M. Weemers, E. A. Pidko, S. Hoffmann, M. Lutz, A. L. Spek, S. C. J. Meskers, R. A. J. Janssen, R. A. van Santen and D. Vogt, *Chem. – Eur. J.*, 2007, **13**, 4548.
- (a) Y. Mao, K. M. H. Lim, Y. Li, R. Ganguly and F. Mathey, *Organometallics*, 2013, **32**, 3562; (b) Y. Hou, Z. Li, Y. Li, P. Liu, C. Y. Su, F. Puschmann and H. Grützmacher, *Chem. Sci.*, 2019, **10**, 3168.
- S. Giese, K. Klimov, A. Mikeházi, Z. Kelemen, D. S. Frost, S. Steinhauer, P. Müller, L. Nyulászi and C. Müller, *Angew. Chem., Int. Ed.*, 2021, **133**, 3625.
- R. J. Newland, M. F. Wyatt, R. L. Wingad and S. M. Mansell, *Dalton Trans.*, 2017, **46**, 6172.
- J. Lin, F. Wossidlo, N. T. Coles, M. Weber, S. Steinhauer, T. Böttcher and C. Müller, *Chem. – Eur. J.*, 2022, e202104135.
- G. Pfeifer, F. Chahdoura, M. Papke, M. Weber, R. Szűcs, B. Geffroy, D. Tondelier, L. Nyulászi, M. Hissler and C. Müller, *Chem. – Eur. J.*, 2020, **26**, 10534.
- M. Rigo, E. R. M. Habraken, K. Bhattacharyya, M. Weber, A. W. Ehlers, N. Mézailles, J. C. Slootweg and C. Müller, *Chem. – Eur. J.*, 2019, **25**, 8769.
- L. Cataldo, S. Choua, T. Berclaz, M. Geoffroy, N. Mézailles, L. Ricard, F. Mathey and P. L. Floch, *J. Am. Chem. Soc.*, 2001, **123**, 6654.
- Only a tetra- $\text{CF}_3$ -substituted diphosphinine is known so far: Y. Kobayashi, H. Hamana, S. Fujino, A. Ohsawa and I. Kumadaki, *J. Am. Chem. Soc.*, 1980, **102**, 252.
- M. H. Habicht, F. Wossidlo, T. Bens, E. A. Pidko and C. Müller, *Chem. – Eur. J.*, 2018, **24**, 944.
- (a) G. Märkl and C. Martin, *Angew. Chem., Int. Ed. Engl.*, 1974, **13**, 408; (b) A. Moores, N. Mézailles, L. Ricard and P. Le Floch, *Organometallics*, 2005, **24**, 508.
- (a) Y. Kobayashi and I. Kumadaki, *Acc. Chem. Res.*, 1978, **11**, 197; (b) T. Ahrens, J. Kohlmann, M. Ahrens and T. Braun, *Chem. Rev.*, 2015, **115**, 931–972; (c) G. Yan, K. Qiu and M. Guo, *Org. Chem. Front.*, 2021, **8**, 3915.
- C. Santamaría, R. Beckhaus, D. Haase, W. Saak and R. Koch, *Chem. – Eur. J.*, 2001, **7**, 622.
- G. O'Mahony and A. K. Pitts, *Org. Lett.*, 2010, **12**, 2024–2027.
- See also: (a) B. Schmid, L. M. Venanzi, A. Albinati and F. Mathey, *Inorg. Chem.*, 1991, **30**, 4693–4699; (b) I. de Krom, E. A. Pidko, M. Lutz and C. Müller, *Chem. – Eur. J.*, 2013, **19**, 7523.
- Please note that the desilylation process was not modelled, but rather the full dehydrofluorination pathway, both with and in the absence of the *ortho*-TMS group, where its presence was not shown to impact the kinetics of triple dehydrofluorination. See ESI† for details.

